The effect of machining defects on the fatigue behaviour of the Al7050 alloy

F. Abroug[1], E. Pessard[1], G. Germain[1], F. Morel[1], E. Chové[2]

[1] LAMPA EA1724–Arts et Métiers ParisTech campus d'Angers, 2 Bd du Ronceray, 49035 Angers – France

[2] Europe Technologies – 2, rue de la Fonderie – B.P. 20536, 44475 CARQUEFOU CEDEX – France

Abstract

During the High Speed Machining (HSM) of aircraft components, geometrical defects, such as mismatches or chatters, can be created. To obtain a high surface quality, an expensive manual grinding operation is systematically done to remove these defects. The aim of this study is to identify the impact of HSM defects on the fatigue behaviour of the aluminium alloy Al7050. After listing and reproducing the most frequently observed surface defects, fatigue tests are conducted under fully reversed plane bending loads. Investigations carried out in previous work showed that residual stresses and the strain hardening introduced by machining under these conditions can be neglected. Therefore, only the geometric aspect of the surface integrity is considered in this study. The results show that the fatigue strength decreases only when the surface roughness is significantly degraded. It is also pointed out that manual grinding allows the effect of the machining defects to be removed from the fatigue behaviour. In order to predict the influence of the surface condition on the fatigue behaviour, a numerical approach based on the real surface topology is also developed. Crack initiation sites that are numerically identified are in agreement with experimental results. Numerical simulation results are compared to the predictions of different fatigue criteria from the literature and discussed over a wide range of surface defects.

Keywords:

Machining defects, fatigue behaviour, aluminium alloy

1 INTRODUCTION

This study is part of a French research project that deals with the control of the machining and grinding of large structural aeronautical components.

The material under investigation is the 7050-T7451 aluminium alloy. During HSM (High Speed Machining) of aircraft parts, macro-geometrical defects can be created. Mismatch may appear due to the gap left between two consecutive passes of the machining tool. Chatter can also be created due to the tool/part vibrations which may occur during different types of machining.

In order to respect the strict specifications imposed by the aeronautical industry, expensive manual grinding is often performed to remove the machining defects.

By the local thermomechanical effects induced, machining can change the surface integrity of manufactured parts and therefore change their fatigue strength. Shahzad [1] and Guillemot [2] showed that changing the cutting conditions can generate a change in surface topology and therefore a change in the fatigue life. Furthermore, Shahzad pointed out that the fatigue resistance shows a significant decrease when surface roughness increases. Even if HSM is known to introduce residual stresses in the machined parts, Tang [3] and Rao [4] showed that these residual stresses are mainly located in the first 50 micrometers below the surface. A variation of the microstructure in the upper surface (hardness variation, grain recrystallization) can also be detected after HSM. Campbell [5] showed that for the Al7000, these changes are located in the first 30 micrometers below the surface.

Different prediction models have been proposed in the literature to take into account the effect of the surface topography on the fatigue strength of machined parts. Analytical models such as [6][7][8] are based on the calculation of the stress concentration factor which is the ratio between the generated and the applied stress in a part. Most of them take into account the sole geometrical aspect of the surface. Numerical approaches also exist and make use of the real surface roughness profile [9][10]. These approaches aim at determining the stress concentration factors at every point of the profile and use them to predict the fatigue behaviour.

The aim of this study is hence to identify the effect of machining defects on the fatigue resistance of a wrought aluminium alloy and to develop a robust prediction method to predict the high cycle fatigue behaviour of a wide range of defects and surface conditions of machined components.

2 MATERIAL AND EXPERIMENTAL METHOD

2.1 Material properties

The specimens were machined out of a 30 mm thick 7050-T7451 aluminum alloy sheet. For this range of thickness, the material shows a high recrystallization rate. Areas of consolidation of recrystallized and non-recrystallized grains can be up to a few millimeters in length. The grains have dimensions ranging from 5 to 300 µm in the L and the TL directions, and 5-50 µm in the TC direction (Figure 1). Different types of intermetallic inclusions are present at the grain boundaries and in the recrystallized grains (Mg_2Si, Al_7Cu_2Fe, $MgZn_2$, AlCuZn, etc …). These inclusions are brittle and can be at the origin of crack initiation under fatigue loading [1].

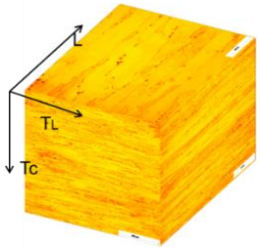

Figure 1: Microstructure of the Al7050-T7451 (L= rolling direction; TL= long transverse; TC= short transverse)

Monotonic tensile tests were conducted to determine the mechanical properties of the material at 0 °, 45 ° and 90 ° to the rolling direction (table 1). The anisotropy of the mechanical behaviour of the studied material is only slight and its ductility is limited with a maximum elongation of 13.9%.

Rolling direction	Rp0.2 [MPa]	Rm [MPa]	Elongation %
0°	475	536	12.3
45°	428	496	13.9
90°	475	538	11.9

Table 1: mechanical properties of the Al7050-T7451.

2.2 Experimental conditions

Fatigue tests were conducted under fully reversed plane bending loads (R=-1). This type of test, via the bending gradient, applies a maximum stress at the top and bottom of the gauge length and thus tends to concentrate the stress on the surface. The specific specimen geometry developed for this study is shown in figure 2. The tests were run on a resonant fatigue testing machine, at a frequency of 75 Hz in plane bending using a Rumul Cracktonic type machine at room temperature and in a ambient air environment. The fatigue tests were conducted using the Stair Case method [11]. 15 samples per batch were used except for the grinded and Ra 4.9µm surface state batches, where 10 specimens were tested. The stopping criterion is the occurrence of a sufficiently long crack (of size greater than 5 mm) detected by a frequency drop of 0.75Hz, or a maximum number of 2.10^6 cycles.

In this project a preliminary study on aircraft components machined by HSM milling was conducted to define different categories of local defects (mismatch, chatter) and degraded surface conditions that may appear by industrial machining. The present work focuses on end milling surface conditions going from the polished state to Ra 4.9µm roughness state and the manually grinded state (table 2).

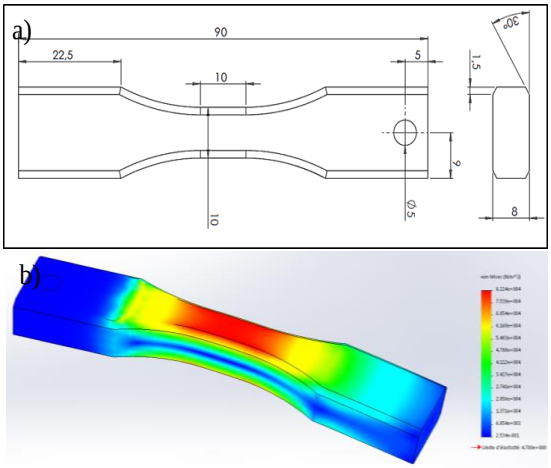

(a) geometry (b) stress distribution when loading

Figure 2: plane bending specimen.

7050-Polished 	7050-Ra2.3 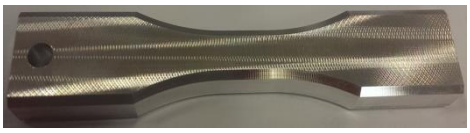
7050-Ra0.6 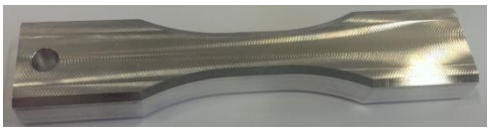	7050-Ra4.9 
7050-grinded 	

Table 2: surface states tested in fatigue.

Polished specimens have been manually polished using abrasive papers ranging from grade 800 to grade 2400. Machining of specimens with a "machined" surface roughness was carried out by end milling (Figure 3). Cutting conditions have been modified in order to obtain different roughness states (table 3). Grinded specimens were prepared by an industrial project partner “Mecachrome” in industrial conditions.

The profiles of these surface roughness states are shown in Figure 4.

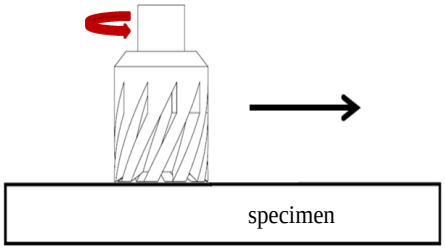

Figure 3: machining strategy for the machined specimens

The studied material has a marked rolling texture and contains a large grain size. Hence, residual stresses characterization by X-ray diffraction analyses is not simple. X-ray analyses were performed on the various surface states. Residual stress analysis provided conclusive results only for the polished and Ra 2.3 µm surface states. The results showed, for these two batches, a small residual tensile stress on the surface that can be neglected.

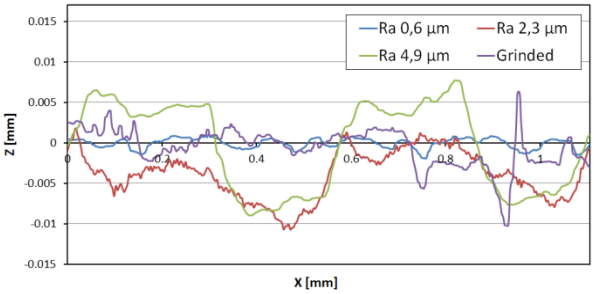

Figure 4: profiles from different test specimen batches

Surface state	N Rotational frequency (rpm)	Fz Feed per tooth (mm/rev)	Z (number of teeth)	Corner radius (mm)	D Diameter of the tool (mm)	Type of tool
Ra 0.6µm	24,000	0.15	4	4	Ø20	solid carbide torus milling cutter with coating
Ra 2.3 µm	24,000	0.55	4	4	Ø20	solid carbide torus milling cutter with coating
Ra 4.9 µm	10,000	0.55	2	0.2	Ø20	milling cutter with uncoating indexable inserts

Table 3: machining conditions the surface states.

Regarding the surface topology, both height and functional parameters [12] were characterized (Table 4). These parameters are:

$$S_a = \frac{1}{S}\iint_S |Z(x,y)|\,dxdy \quad (1)$$

$$S_q = \sqrt{\frac{1}{S}\iint_S \left(Z(x,y)\right)^2 dxdy} \quad (2)$$

$$S_{ku} = \frac{1}{S_q^4}\left(\frac{1}{S}\iint_S \left(Z(x,y)\right)^4 dxdy\right) \quad (3)$$

$$S_{vi} = \frac{1}{S_q}\frac{V_v(h_{0.8})}{S} \quad (4)$$

where: Sa = arithmetic mean height; Sq = Root mean squared height; Sku = Kurtosis; S_{vi} = groove’s fluid retention index and $Vv(h_{0.8})$ = The void volume of the valley section that represents 80% of the material ratio curve [13].

3 RESULTS AND DISCUSSIONS

Fatigue tests highlight the effect of each surface condition on the fatigue strength. The results are shown in table 4. Unbroken specimens from the staircase fatigue test have been tested at a higher load in order to characterize the S-N curve trend (Figure 5).

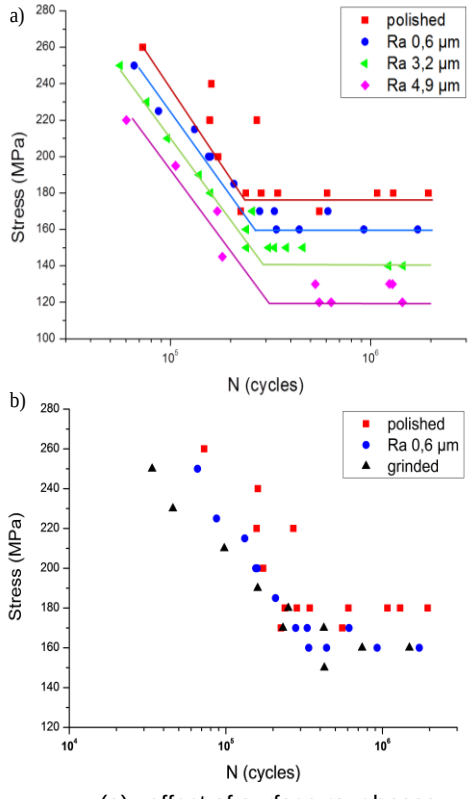

(a) effect of surface roughness
(b) manual grinding on fatigue limit

Figure 5: S-N curves of Al7050 under plane bending load.

Surface state	Sa [µm]	Sku	Sq [µm]	Svi	Kf	σ_D [MPa] (experimental)	σ_D [MPa] (calculated)
polished	≤0.04	3.55	≤0.05	0.12	1	174	174
Ra 0.6	1.106	2.499	1.187	0.088	1.026	160	169.6
grinded	3.839	2.768	4.54	0.087	1.109	157	156.8
Ra 2.3	4.243	7.36	6.414	0.051	1.241	141	140.24
Ra 4.9	5.511	1.943	5.74	0.042	1.047	119	164.81

Table 4: results of the experimental tests and prediction of fatigue limit.

Most studies on the effect of surface geometry on fatigue strength propose criteria based on the usual roughness parameters (Ra, Rz) [6][7]. The main shortcomings of these criteria stem from the fact that they are all based on a profile measured over a line. It is difficult to extrapolate these criteria to heterogeneous surface conditions (such as shown in Figure 6) that can be obtained by milling. The use of height and functional parameters presented above seems to be more suitable.

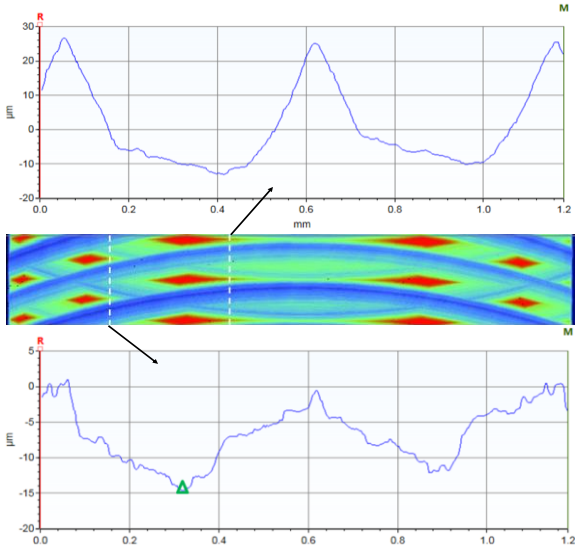

Figure 6: variation of the obtained pattern depending on the measurement position.

Evolution of the fatigue limit based on the arithmetic mean height of its surface S_a is shown in Figure 7.

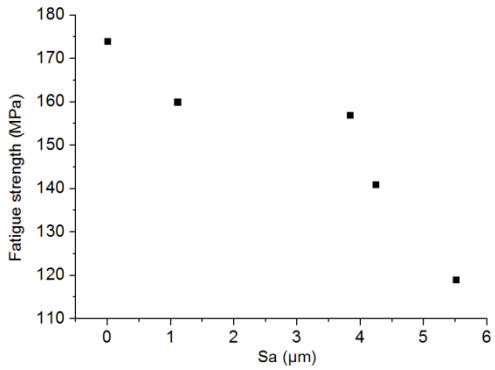

Figure 7: fatigue limit evolution as a function of S_a.

According to Figure 7, the Sa parameter seems to correlate with the fatigue behaviour of the different tested batches. The endurance limit decreases slowly for the low values of Sa then drops sharply when Sa exceeds a threshold value of 3.5µm.

The approach proposed by Souto-Lebel [8] is one of the few approaches based on surface parameters rather than parameters measured over a line. It is based on the calculation of the effective stress concentration factor dependent on several surface parameters:

$$K_f = 1 + S_{vi} \cdot S_{ku} \cdot \frac{S_q}{a_c} \quad (5)$$

Where a_c is a critical defect size which can be determined by readjustment. The fatigue limit of machined specimens is then predicted by referring to the fatigue limit of a flawless surface material, in this case the polished state:

$$\sigma_{D_{machined}} = \frac{\sigma_{D_{polished}}}{K_f} \quad (6)$$

The critical defect size a_c chosen to minimize the prediction errors for the different batches is 10 µm. The results are shown in Table 4. Figure 8 shows the comparison of the predictions obtained by this approach and the experimental results.

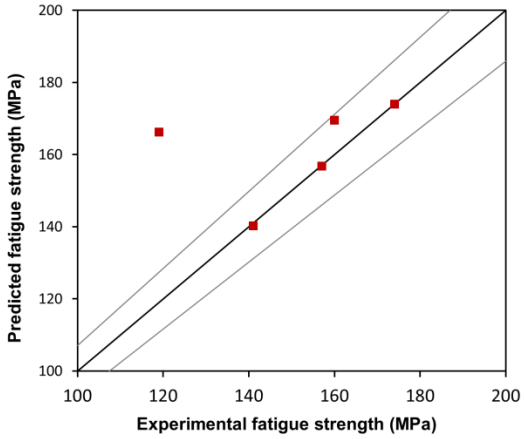

Figure 8: comparison between experimental results and Souto-Lebel's approach predictions.

According to Figure 8, Souto-Lebel's approach is efficient for the 4 batches with the lowest roughness. The maximum error is then less than 7%.

However, the prediction of the fatigue limit for the Ra4,9 surface condition is too optimistic.

Another approach based on finite element (FE) simulations has been developed in order to better take into account the stress distribution at the bottom of the machining grooves for any surface states and surface defect. In this new approach, the surface topology is experimentally characterized using a BRUCKER Contour GTK0-X type of profilometer.

A regular Gaussian regression filter is then applied over the scanned surface profile to remove undesired

singularities. The filter is a long wavelength pass filter with a short wavelength cutoff of 15µm. The obtained surface is then modelled using the finite element method (Figure 9). An elastic calculation is performed. The finite elements used are tetrahedral with reduced integration and are of a size of 3.5µm on the surface. The boundary conditions are as follows:

- U1=0 along of the plane X_0(surface A).
- U2=0 along of the line X_0,Y_0.
- U3=0 at the point X_0,Y_0,Z_0.
- a bending pressure function is applied along the surface B.

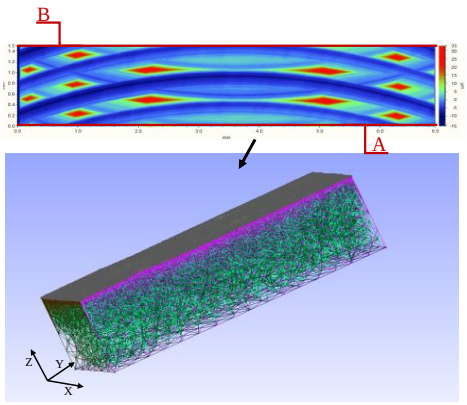

Figure 9: FE model based on the actual surface topography of machined specimen.

It is shown that the location of the maximum stress values from the FE analysis are in good agreement with the locations of the crack initiation locations experimentally observed on the tested specimens (Figure 10). Figure 10-a shows the presence of a non-metallic inclusion at the crack initiation site of a machined specimen. The generated stress is mainly in X direction.

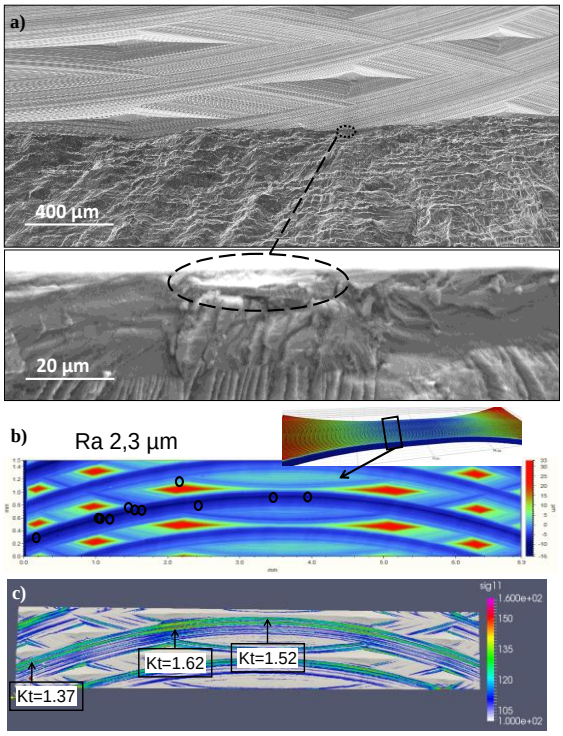

(a) crack initiation site (b) experimental locations of initiation (c) FE analysis.

Figure 10: comparison between experimental results and FE analysis.

The stress concentration factor K_t which represents the ratio between the generated and the applied stress is not homogeneous for the Ra2.3µm surface condition. K_t goes from 1.37 near the specimen's border, to 1.52 in the centre and 1.6 in the most critical zone. This zone is located at 1.3 mm from the specimen's centre and spreads over 0.8 mm of width.

From the comparison between crack initiation sites from Figure 10-b and the stress concentration zones from the FE analysis in Figure 10-c it is clear that crack initiation is located in the machining grooves with high stress concentration factor K_t but not necessarily in the zones where K_t is maximum. This means that the local stress intensity is one of the most significant parameters in the crack initiation mechanism but the macroscopic fatigue strength may also depend on the extent of the loaded zone.

The maximal stress concentration factor $K_{t\ max}$ is measured as well by FE analysis for the surface conditions Ra 0.6µm, Ra 2.3µm and Ra 4.9µm. The stress concentration factor for the polished surface condition is taken as equal to 1. Results of the fatigue limit as a function of $K_{t\ max}$ are shown in Figure 11. Again, the relation between the localized maximal stress concentration factor $K_{t\ max}$ and the fatigue behaviour for the milled surfaces is not that clear.

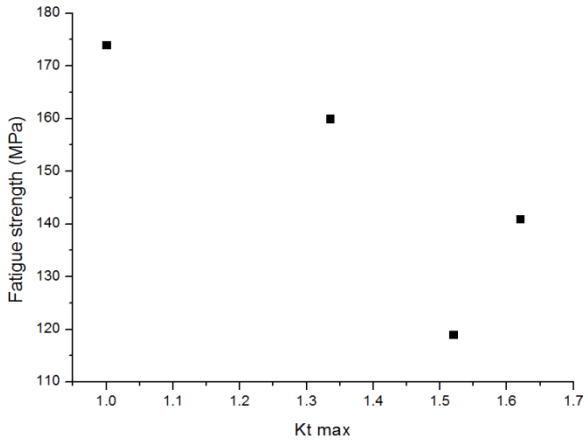

Figure 11: fatigue limit as a function of maximal stress concentration factor based on FE analysis.

In an ongoing investigation, a multiaxial endurance criterion using the stress fields computed by FE simulations from real scan surfaces is being built and used to predict the fatigue behaviour of the Al7050 in presence of different surface conditions and defects. This criterion must take into account the global aspect of surface geometry since local criteria don't seem to provide the good tendencies.

4 CONCLUSION

From the results of a vast experimental fatigue campaign carried out in plane bending on the aeronautical aluminium alloy Al7050-T7451 showing different surface profiles, the following conclusions can be drawn:

1. The height parameter Sa is correlated with the fatigue limit of the different tested batches. When the arithmetic mean height Sa is greater than 3.5µm the fatigue limit decreases more sharply.

2. The manual grinding operation provides a fatigue limit as good as a classical aircraft machining roughness (Ra 0.6µm).
3. The localization of the crack initiation zones is in agreement with the high stress areas identified by numerical computation.
4. In addition to the local stress intensity, the macroscopic fatigue strength may depend on the extent of the loaded zone.

5 ACKNOWLEDGMENTS

This work was carried out within the FUI QUAUSI project with the support of industrial (Dassault Aviation, Europe Technologie, Figeac Aéro, Mecachrome, Spring Technologie, Precise, GEBE2, CETIM) and academic partners (IRCCyN-IUT Carquefou).

6 REFERENCES

[1] Shahzad, M., Chaussumier, M., Chieragatti, R., Mabru, C., Rezai Aria, F., 2010, Influence of anodizing process on fatigue life of machined aluminium alloy, Procedia Engineering, 2: 1015–1024.

[2] Guillemot, N., 2010, Prise en compte de l'intégrité de surface pour la prévision de la tenue en fatigue de pièces usinées en fraisage, PhD Thesis, ENS Cachan.

[3] Tang, Z.T, Liu, Z.Q, Pan, Y.Z, Wan, Y., Ai, X., 2009, The influences of tool flank wear on residual stresses induced by milling aluminum alloy, Journal of Materials Processing Technology, 209: 4502–4508.

[4] Rao, B., Shin, Y.C, 2001, Analysis on high-speed face-milling of 7075-T6 aluminum using carbide and diamond cutters, International Journal of Machine Tools & Manufacture, 41: 1763-1781.

[5] Campbell, C.E., Bendersky, L.A., Boettinger, W.J, Ivester, R., 2006, Microstructural characterization of Al-7075-T651 chips and work pieces produced by high-speed machining, Materials Science and Engineering, A 430: 15–26.

[6] Arola, D., Williams, C.L., 2002, Estimating the fatigue stress concentration factor of machined surfaces, International Journal of Fatigue, 24:923-930.

[7] Neuber, H., 1961, Theory of Stress Concentration for Shear-Strained Prismatical Bodies With Arbitrary Nonlinear Stress-Strain Law, Journal of Applied Mechanics; 28:544.

[8] Souto-Lebel, A., 2014. Rôle de l'intégrité de surface dans la tenue en fatigue d'un acier bainitique après fraisage de finition, PhD Thesis, Cachan: ENS Cachan.

[9] Suraratchaï, M., Limido, J., Mabru, C., Chieragatti, R., 2008. Modelling the influence of machined surface roughness on the fatigue life of aluminium alloy. International Journal of Fatigue, 30:2119,2126.

[10] Ås, S. K., Skallerud, B., Tveiten, B. W., 2008. Surface roughness characterization for fatigue life predictions using finite element analysis, International Journal of Fatigue, 30:2200,2209.

[11] Little, R.E., Jebe, E.H., 1975. Statistical Design of Fatigue Experiments. applied science publishers Ltd., London.

[12] Griffiths, B., 2001. Manufacturing Surface Technology: Surface integrity and Functional Performance. London: Prenton Press.

[13] Leach, R. K., 2013. Characterisation of areal surface texture. Berlin: Springer.